STABILITY OF G^+ MODES IN A 30 $M_\odot$ STAR

R. SCUFLAIRE, A. NOELS, M. GABRIEL, and A. BOURY
Institut d'Astrophysique de l'Université de Liège,
Liège, Belgique

(Received 15 May, 1975)

Abstract. The evolution of a Population I 30 $M_\odot$ star has been computed during the Main Sequence phases without taking semi-convection into account. These models have a temperature gradient larger than the adiabatic value in the inhomogeneous region. The models have been tested for stability towards g^+ modes of non-radial oscillations to see whether Kato's mechanism leads to an instability. Whereas the models are stable during the early Main Sequence phases, they become unstable for low enough central hydrogen abundance.

1. Introduction

Kato (1966) suggested that in a region of varying molecular weight, some mixing takes place, due to vibrational instability, as soon as the temperature gradient $\nabla_T = (\mathrm{d} \ln T/\mathrm{d} \ln p)$ exceeds the adiabatic value $\nabla_{a,T} = (\Gamma_2 - 1/\Gamma_2)$. When the Main Sequence phases are computed ignoring semi-convection, stars of mass larger than 10 $M_\odot$ develop a region of inhomogeneous chemical composition where $\nabla_T > \nabla_{a,T}$ (Tayler, 1969; Gabriel, 1970). According to Kato, overstability will produce a partial mixing of material in the inhomogeneous region this will reduce the μ gradient in such a way that $\nabla_T = \nabla_{a,T}$.

However, Kato's discussion is strictly local and before concluding to any instability, the influence of the other layers of the star must be taken into account. This was attempted by Gabriel (1969) and by Aure (1971) for asymptotic modes. The aim of this work is to verify whether an instability arises for low order g^+ modes. We find that sufficiently evolved Main Sequence models are indeed unstable for values of the degree of spherical harmonics l equal to 1 and 2. Stability is, however, restored for $l=2$ at the very end of central hydrogen burning because the superadiabatic region is then separated from the convective core by a more and more extended stabilizing layer with a subadiabatic temperature gradient. Preliminary results were published earlier (Gabriel *et al.*, 1975a). They are slightly modified following improvements in the numerical method of integration for the more evolved models (see Section 3).

2. The Models

The evolution of a 30 $M_\odot$ star with $X=0.602$, $Z=0.04$ was started during the gravitational contraction just before the onset of the CNO cycle and carried on until the end of central hydrogen burning. Semi-convection was ignored. Therefore during the Main Sequence phases the models are composed of 5 zones shown schematically in Figure 1:

Astrophysics and Space Science **39** (1976) 463–475.

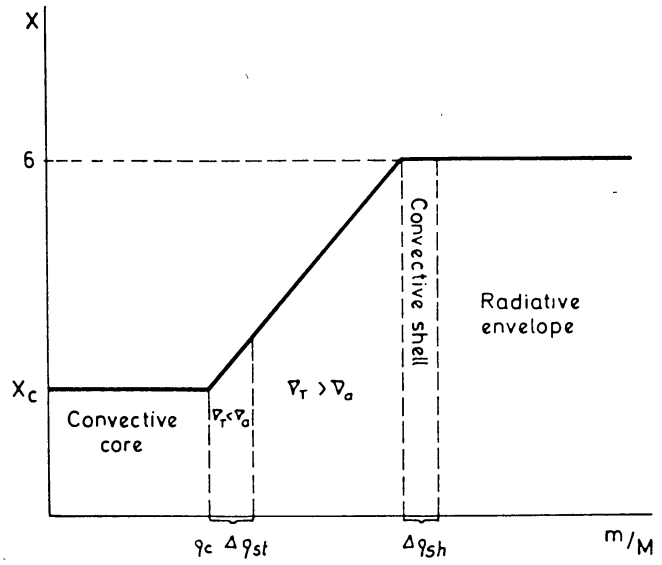

Fig. 1. Schematic hydrogen profile and the five zones of the models.

a convective core of mass fraction q_C, a shell of mass Δq_{st} where $\nabla_T < \nabla_{a,T}$, another inhomogeneous region where $\nabla_T > \nabla_{a,T}$, a convective layer of mass fraction Δq_{sh} and the outer radiative envelope. The mass fraction at the bottom of the convective shell is 0.635, that is the extension of the convective core on the Z.A.M.S.

In evolved model this point is not convectively neutral but the region just beneath is stabilized against convection by the μ gradient. Therefore,

$$\nabla_{a,T} < \nabla_T < \nabla_{a,T} + \left(\frac{\partial \ln T}{\partial \ln \mu}\right)_{\varrho,p} \frac{\mathrm{d} \ln \mu}{\mathrm{d} \ln p}.$$

Table I gives some properties of the models: the age t, the central hydrogen abundance X_C, the central concentration $\varrho_C/\bar{\varrho}$, q_C, Δq_{st} and Δq_{sh} defined above, the bolometric magnitude M_{Bol} and the effective temperature T_{eff}. It shows that Δq_{st} is zero or very small during most of the Main Sequence phases and that it increases steeply as models approach exhaustion of central hydrogen.

3. Non-Radial Adiabatic Oscillations

The fourth order system of differential equations of non-radial adiabatic oscillations and the boundary conditions imposed are given in Boury *et al.* (1975). The principle of the method remains the same here. However, the integration procedure has been modified in order to improve the accuracy of the eigenfunctions for highly condensed models. The number of points in the models has also been increased.

Several test computations were carried out using different integration schemes: Runge-Kutta type methods, Taylor expansions of various orders and a difference

method. The difference method proved to be the most stable for highly condensed models. The difference equations were written as

$$\frac{\mathbf{y}_{i+1} - \mathbf{y}_i}{x_{i+1} - x_i} = \tfrac{1}{2}(A_{i+1}\mathbf{y}_{i+1} + A_i\mathbf{y}_i), \tag{1}$$

where A stands for the matrix of the coefficients in the right-hand members of the system, $\mathbf{y}$ the vector composed of the unknown function and x the independent variable.

4. Vibrational Stability

In the first order approximation, non-conservative terms introduce a damping factor of the form $\exp[-\sigma' t]$.

The coefficient of vibrational stability σ' is given by (Gabriel *et al.*, 1975b)

$$\sigma' = \frac{\int_0^{M_a} \frac{\delta T}{T}\left\{-\delta\varepsilon + \frac{\mathrm{d}(\delta L_R^r + \delta L_C^r)}{\mathrm{d}m} + \frac{l(l+1)}{r^2} \times \right.}{2\sigma_a^2 \int_0^M \left[\delta r^2 + \frac{l(l+1)}{\sigma_a^4 r^2}\chi^2\right] \mathrm{d}m} \tag{2}$$

$$\left. \times \left[\frac{-\delta F_{\theta,R} - \delta F_{\theta,C}}{\varrho} - \frac{\chi}{\sigma_a^2}\frac{\mathrm{d}L}{\mathrm{d}m} + \frac{\chi}{\sigma_a^2}\frac{F}{\varrho r}\right]\right\} \mathrm{d}m$$

$$= \frac{N}{D} = I_\varepsilon + I_{R,r} + I_{C,r} + I_{R,nr} + I_{C,nr} + I_L + I_F, \tag{3}$$

where the I's correspond to the various terms in Equation (2).

In that equation δ is the symbol for the Lagrangian perturbation. The perturbation of the flux F has the components

$$\delta F^r = \delta F^r Y_l^m, \qquad \delta F^\theta = \frac{\delta F_\theta}{r^2}\frac{\partial Y_l^m}{\partial\theta}, \qquad \delta F^\varphi = \frac{\delta F_\theta}{r^2 \sin^2\theta}\frac{\partial Y_l^m}{\partial\varphi},$$

Y_l^m being the spherical function of degree l and order m.

The notation δL^r is used for

$$\frac{\delta L^r}{L} = 2\frac{\delta r}{r} + \frac{\delta F^r}{F}.$$

The subscripts R and C refer to the radiative and the convective fluxes. We also have

$$\chi = \delta\Phi + \frac{p}{\varrho}\frac{\delta p}{p},$$

Φ being the gravitational potential. The integration limit M_a is taken as the point where

$$\frac{\Gamma_2 - 1}{\Gamma_2}\frac{\delta p}{p} = \frac{1}{\sigma_a C_p T}\delta\left[\varepsilon - \frac{1}{\varrho}\nabla\cdot\mathbf{F}\right].$$

For $m > M_a$ the adiabatic approximation is no longer valid and these layers are supposed not to contribute to the damping coefficient (Ledoux and Walraven, 1958). The expressions for the perturbation of the convective and radiative flux are given in Gabriel *et al.* (1975b).

In the radiative region it is useful to combine the fourth and the last terms in Equation (2) to write

$$D(I_{R,nr} + I_F) = \int \frac{\delta T}{T} \frac{l(l+1)}{\varrho r^2} \left(-\delta F_{\theta,R} + \frac{\chi}{\sigma_a^2} \frac{F}{r} \right) \mathrm{d}m =$$

$$= -\int \frac{\delta T}{T} L \frac{l(l+1)}{r^2} \left[\frac{\dfrac{\delta T}{T}}{\dfrac{\mathrm{d} \ln T}{\mathrm{d}r}} - \delta r \right] \mathrm{d}r. \tag{4}$$

By use of

$$\frac{\delta T}{T} = \nabla_{a,T} \left[\frac{p'}{p} + \frac{\mathrm{d} \ln p}{\mathrm{d}r} \delta r \right],$$

p' being the Eulerian perturbation of the pressure, Equation (4) becomes

$$D(I_{R,nr} + I_F) = -\int \frac{\delta T}{T} \frac{l(l+1)}{r^2} L \left[\nabla_{a,T} \frac{p'}{p} \left(\frac{\mathrm{d} \ln T}{\mathrm{d}r} \right)^{-1} + \right.$$

$$\left. + \frac{\nabla_{a,T} - \nabla_T}{\nabla_T} \delta r \right] \mathrm{d}r. \tag{5}$$

It is also interesting to write δL_R^r as

$$\frac{\delta L_R^r}{L_R} = 2 \frac{\delta r}{r} + \left(4 - \frac{\partial \ln \varkappa}{\partial \ln T} \right) \frac{\delta T}{T} - \left(1 + \frac{\partial \ln \varkappa}{\partial \ln \varrho} \right) \frac{\delta \varrho}{\varrho} +$$

$$+ \frac{\nabla_{a,T}}{\nabla_T} \left[\frac{\delta p}{p} - \frac{\delta \varrho}{\varrho} - \frac{1}{g} \frac{\mathrm{d}\Phi'}{\mathrm{d}r} + \left(2 + \frac{\sigma_a^2 r^3}{Gm} - \frac{4\pi G \varrho r}{g} \right) \frac{\delta r}{r} \right] +$$

$$+ \frac{\mathrm{d} \nabla_{a,T}}{\mathrm{d} \ln T} \frac{\delta p}{p} + \frac{\nabla_{a,T} - \nabla_T}{\nabla_T} \frac{\mathrm{d} \delta r}{\mathrm{d}r}. \tag{6}$$

On the other hand, for the high-order modes considered in Kato's approximation, all perturbations take the form $\exp(i\mathbf{k} \cdot \mathbf{r})$. Then, $\nabla F' \simeq F \nabla^2 T' / (\mathrm{d}T/\mathrm{d}r) = -k^2 F T' / (\mathrm{d}T/\mathrm{d}r)$ and the numerator of σ' becomes

$$N = -\int \frac{\delta T}{T} L \left[k_r^2 + k_H^2 \right] \left[\nabla_{a,T} \left(\frac{\mathrm{d} \ln T}{\mathrm{d}r} \right)^{-1} \frac{p'}{p} + \frac{\nabla_{a,T} - \nabla_T}{\nabla_T} \delta r \right] \mathrm{d}r \tag{7}$$

where k_r and k_H are the vertical and horizontal wave numbers. Making div $\delta \mathbf{r} = 0$ as in Kato's work, one can also write D as

$$D = 2\sigma_a^2 \int_0^M (\delta \mathbf{r})^2 \, \mathrm{d}m = 2\sigma_a^2 \int_0^M (\delta r)^2 \frac{k^2}{k_H^2} \, \mathrm{d}m. \tag{8}$$

Equations (7) and (8) yield the same expression of σ' as derived from Kato's dispersion equation. Since for high overtones $p' \simeq 0$ and $\delta T\, \delta r < 0$ a layer for which $\nabla_T > \nabla_{a,T}$ contributes to instability ($\sigma' < 0$).

The non-radial term in Equation (7) compares immediately with Equation (5) if one makes the correspondence $l(l+1)/r^2 \to k_H^2$. However, Equation (6) shows that the radial term in Equation (7) is hidden in the second member of Equation (2). The correspondence $\mathrm{d}^2\, \delta r/\mathrm{d}r^2 \to k_r^2\, \delta r$ shows that the radial term in Equation (7) corresponds to the last term of Equation (6). All the other terms of that equation are negligible for the high overtones considered by Kato but not for low order g modes.

The four models whose properties are given in Table I were checked for stability towards the first g^+ modes for degrees of spherical harmonic $l=1$ and 2. The results are summarized in Tables II ($l=1$) and III ($l=2$). Both models 3 and 4 are unstable, with respect to the g_4 mode. Model 3 is unstable both for $l=1$ and 2 while model 4 is unstable for $l=1$.

TABLE I

A few properties of the models

No.	1	2	3	4
t (yr)	1.620(4)	1.623(6)	2.874(6)	3.570(6)
X_C	0.595	0.410	0.182	0.001
$\varrho_C/\bar{\varrho}$	30.4	56.75	167	667
q_C	0.5908	0.4881	0.3916	0.3218
Δq_{st}	0	0	0.0134	0.0666
Δq_{sh}	0	510^{-3}	0.0137	0.0372
M_{Bol}	−8.208	−8.446	−8.674	−8.862
log T_{eff}	4.6263	4.5992	4.5534	4.5443

TABLE II

Periods of oscillations (P) and e-folding times σ'^{-1} for $l=1$

No.		1	2	3	4
g_1	P (s)	6.108(4)	4.298(4)	3.322(4)	3.2594(4)
	σ'^{-1} (yr)	3.771(3)	1.133(4)	2.023(3)	2.884(0)
g_2	P	9.665(4)	8.303(4)	7.612(4)	3.784(4)
	σ'^{-1}	6.706(2)	2.655(3)	9.642(3)	1.103(2)
g_3	P	1.316(5)	1.256(5)	1.049(5)	6.003(4)
	σ'^{-1}	1.196(2)	8.496(2)	2.904(3)	8.147(3)
g_4	P	1.670(5)	1.576(5)	1.389(5)	8.441(4)
	σ'^{-1}	2.827(1)	5.340(2)	−3.756(4)	−8.437(4)
g_5	P				1.021(5)
	σ'^{-1}				3.408(3)

TABLE III

Periods and e-folding times for $l=2$

No.		1	2	3	4
g_1	P (s)	3.802(4)	2.776(4)	2.852(4)	2.508(4)
	σ'^{-1} (yr)	2.547(3)	7.040(3)	4.965(0)	7.884(−2)
g_2	P	5.815(4)	5.038(4)	4.592(4)	3.351(4)
	σ'^{-1}	4.733(2)	1.781(3)	7.129(3)	1.651(0)
g_3	P	7.802(4)	7.460(4)	6.439(4)	3.556(4)
	σ'^{-1}	9.7901(1)	5.840(2)	1.700(3)	3.028(1)
g_4	P	9.830(4)	9.258(4)	8.193(4)	4.982(4)
	σ'^{-1}	2.480(1)	4.199(2)	−1.612(5)	6.528(4)
g_5	P	–	1.082(5)	9.976(4)	6.285(4)
	σ'^{-1}		1.517(2)	7.886(2)	3.001(3)
g_6	P	–	1.306(5)	1.101(5)	6.809(4)
	σ'^{-1}		4.743(1)	+2.485(3)	2.619(3)

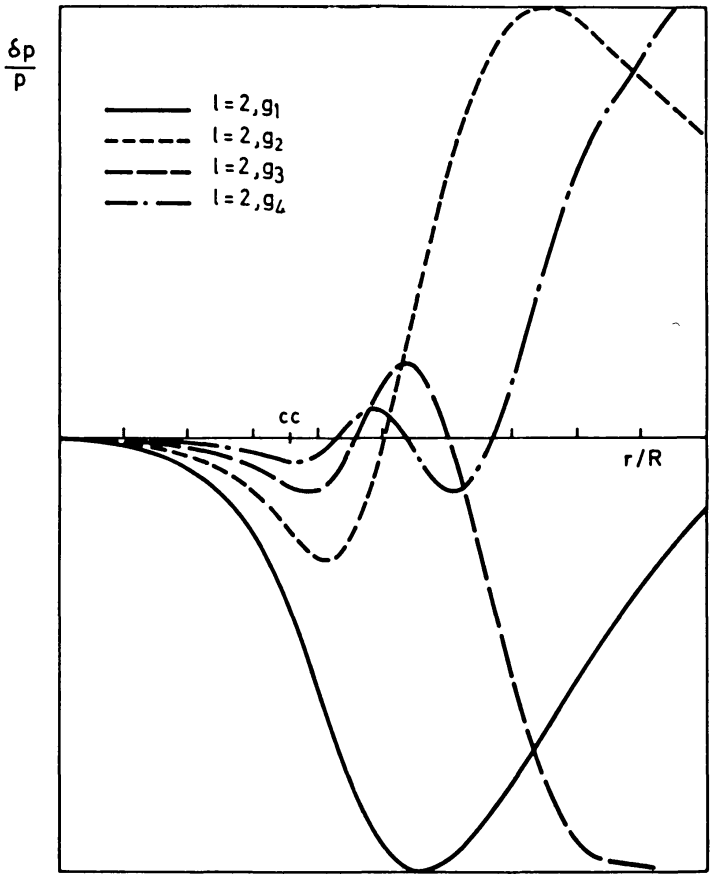

Fig. 2. $\delta p/p$ for the 4 first g^+ modes ($l=2$) of the Z.A.M.S. model distance to the center. $\delta p/p$ is in arbitrary units. Label cc indicates the surface of the convective core.

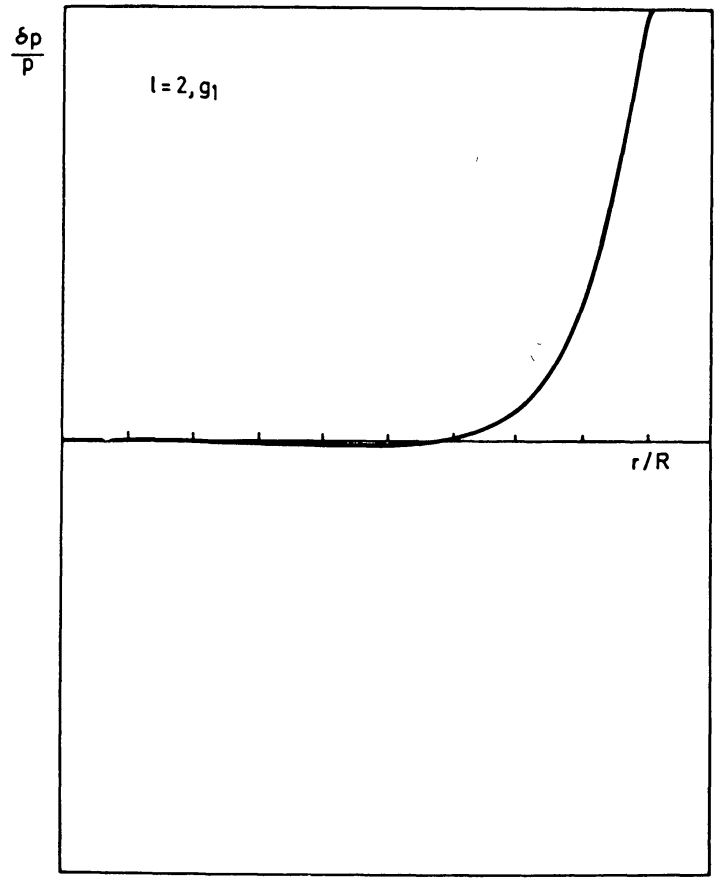

Fig. 3. $\delta p/p$ for the g_1^+ mode $l=2$ of model 4.

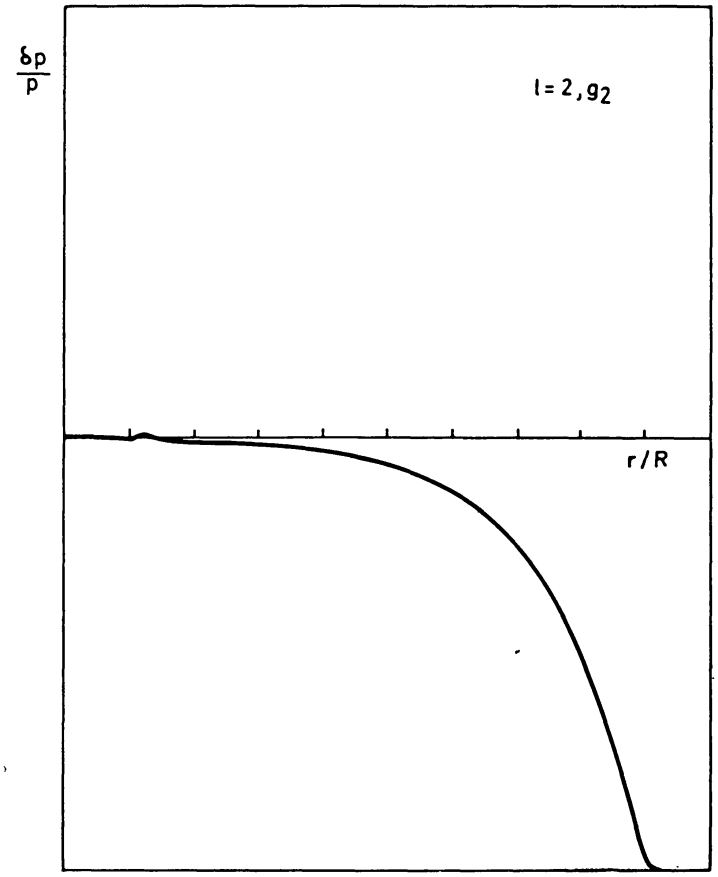

Fig. 4. $\delta p/p$ for the g_2^+ mode, $l=2$, of model 4.

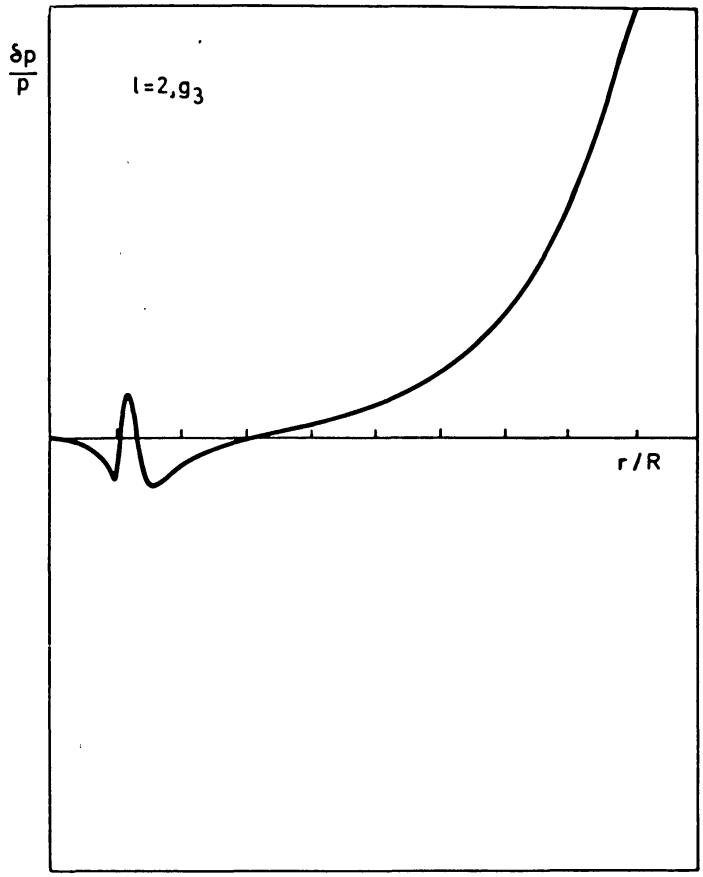

Fig. 5. $\delta p/p$ for the g_3^+ mode, $l=2$, of model 4.

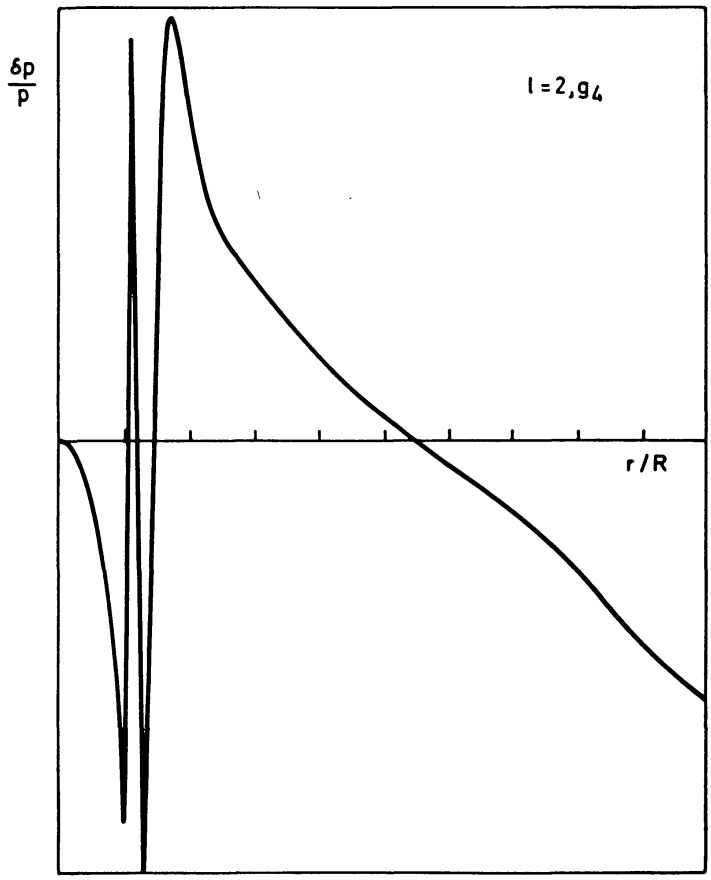

Fig. 6. $\delta p/p$ for the g_4^+ mode, $l=2$, of model 4.

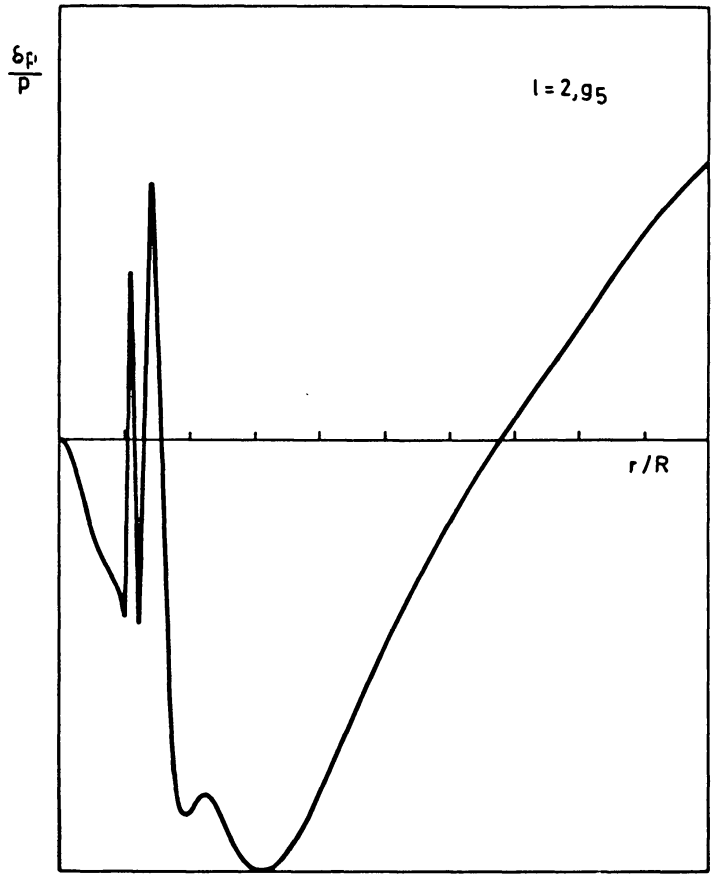

Fig. 7. $\delta p/p$ for the g_5^+ mode, $l=2$, model 4.

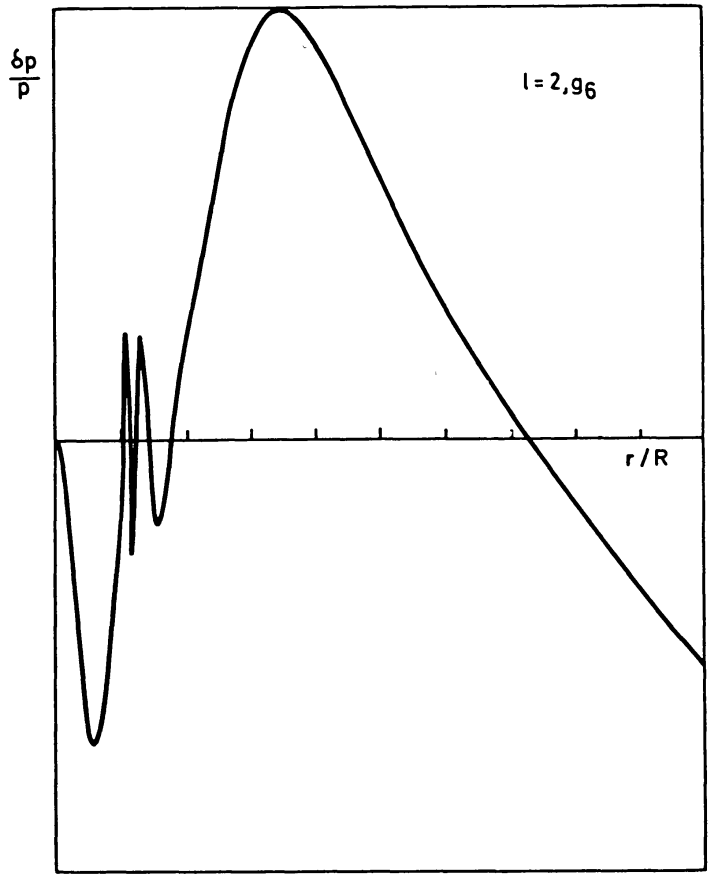

Fig. 8. $\delta p/p$ for the g_6^+ mode, $l=2$, of model 4.

The behaviour of the eigenfunction $\delta p/p$ is given for the first g^+ modes in Figure 2 for model 1 and in Figures 3 to 8 for model 4 in both cases for $l=2$. These figures show the drastic modifications of the eigenfunctions due to evolution. In model 1, the amplitudes in the convective core and just above become smaller and smaller compared to the surface value as the order of the mode increases. On the contrary in model 4, the amplitudes in the convective core and in the inhomogeneous region where most of the nodes are located at first increase with the order of the mode compared to the surface value. For modes higher than g_4 however the situation is reversed. The accumulation of the nodes just above the convective core can be understood by the fact that, in the interior of a star, the amplitude of the g^+ modes can have an oscillatory character only in the region where $\sigma_a^2 < -Ag$, with $A = \mathrm{d} \ln \varrho/\mathrm{d}r - (1/\Gamma_1)(\mathrm{d} \ln p/\mathrm{d}r)$ (Scuflaire, 1974). Figure 9 gives Ag vs r/R for models 1 (full line) and 4 (dotted line). Clearly, the allowed region for oscillatory amplitudes narrows more and more when evolution proceeds.

Since the destabilizing mechanisms operate in the deep interior of the star, i.e. the

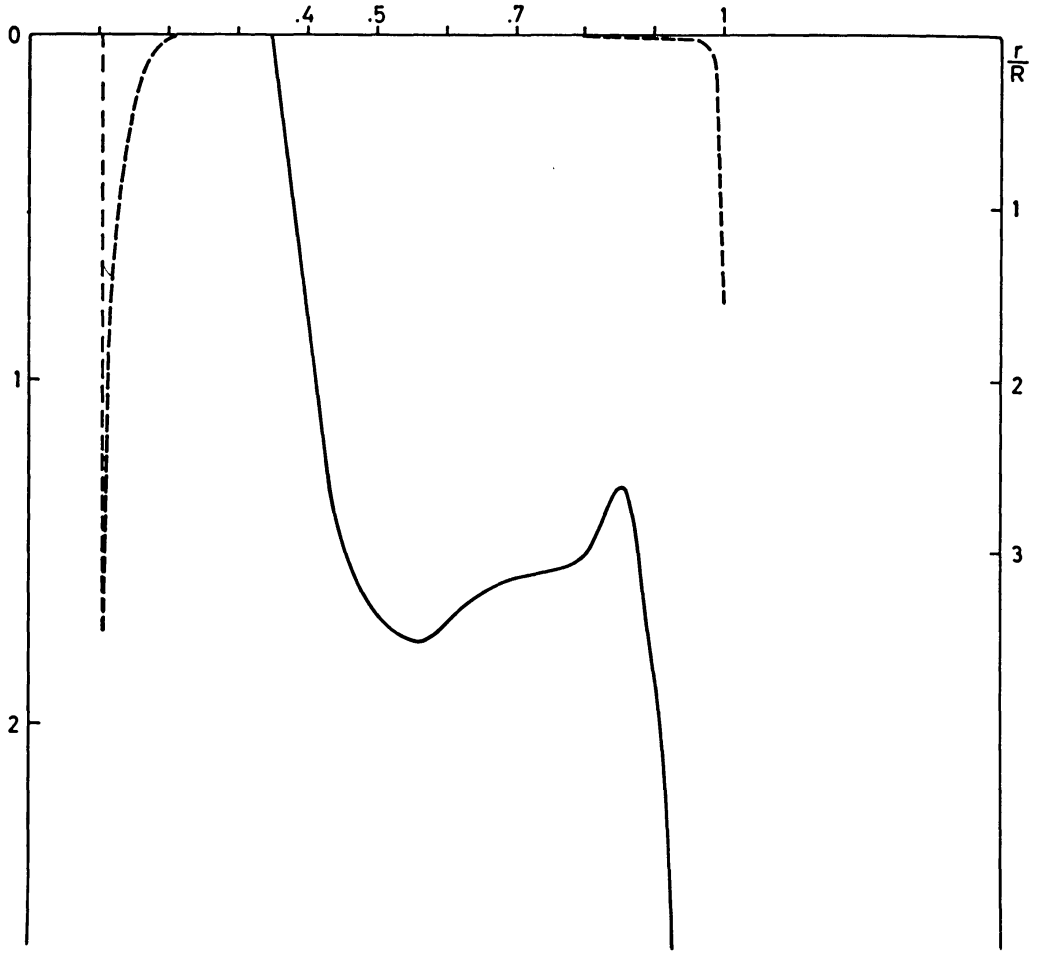

Fig. 9. $Ag = -N^2$, N being the Väisälä frequency, vs the distance from the center for models 1 (full line and scale at the right) and 4 (dotted line and scale at the left). Ag is in unit 10^{-7} cgs.

nuclear burning region and the chemically inhomogeneous zone, an instability is most likely to occur in evolved models for the g_4 mode. For early Main Sequence models the amplitudes in the destabilizing zones are too small and the region with $\nabla_T > \nabla_{a,T}$ is also smaller than in the more evolved ones.

This does not mean that each point of the radiative homogeneous envelope is damping. For instance we encounter eigenfunctions (see Figure 8) which have an extremum in the envelope. Clearly after the extremum, the radial component of the perturbed luminosity δL_R^r decreases outwards, which has a destabilizing influence. However the effect of that term taken globally over the envelope is always stabilizing.

The presence of such an extremum in $\delta p/p$ results from the following. For early Main Sequence models $\delta p/p$ and $\delta r/r$ have generally opposite signs in the interior but because $\delta p/p$ has one node less than $\delta r/r$ they have the same sign in the other region. This was also found by Smeyers (1966). However, during the Main Sequence phases $\delta p/p$ acquires one extra node changing its sign at the surface. This occurs first for the g_1 mode and then for progressively higher harmonics. As a result of this behaviour of $\delta p/p$, the terms given in Equation (5) which during the early Main Sequence phases have a stabilizing influence in the outer envelope later become driving for an increasing number of harmonics as

$$\left|\frac{\delta r}{r}\right| > \left|\frac{\delta T}{T}\frac{\mathrm{d}\ln r}{\mathrm{d}\ln T}\right|.$$

However, for low l values this effect remains too small to produce an instability.

Let us return to Equations (5) and (6) which isolate Kato's terms. For the harmonics g_3 and higher, the eigenfunctions behave practically like asymptotic modes above the convective core where the nodes are accumulating. As a result $\delta T/T\,\delta r/r < 0$ and p'/p is small ($p'/p \lesssim 10^{-2}\,(\delta p/p)$). However $\nabla_T - \nabla_{a,T}$ also is small ($< 1.210^{-2}$) in the inhomogeneous region and it is not *a priori* obvious that, on the whole, $\delta L_R^r/L_R^r$ and Equation (5) will contribute to instability there. Fortunately, p'/p has always the same sign as $\delta r/r$ in that region and this reinforces the destabilizing effect of the term $(\nabla_{a,T} - \nabla_T)\delta r$ in Equation (5). The situation is still more critical when one considers Equation (7). $(\delta T/T)(\mathrm{d}\delta L_R^r/\mathrm{d}m)$ changes sign roughly at each extremum. The overall effect in the region where $\mathrm{d}\mu/\mathrm{d}r \neq 0$ is nevertheless destabilizing except in the case of model 4. For this model the stabilizing influence of the zone Δq_{st} (see Figure 1) is large enough to overcome the destabilizing effect of the rest of the inhomogeneous region.

Table IV gives in a few cases the I's defined in Equation (3) and

$$I_{R,r}^{u} = \int \frac{\delta T}{T}\frac{\mathrm{d}\delta L_R^r}{\mathrm{d}m}\,\mathrm{d}m/D,$$

$$I_{R,nr}^{u} = -\int \frac{\delta T}{T}\frac{l(l+1)}{r^2}L\left[\frac{\dfrac{\delta T}{T}}{\dfrac{\mathrm{d}\ln T}{\mathrm{d}r}} - \delta r\right]\mathrm{d}r/D,$$

TABLE IV

Supplementary data concerning σ' for selected modes

Model No.	2	3			4				
mode	$l=2, g_1$	$l=1, g_4$	$l=2, g_4$	$l=2, g_5$	$l=1, g_4$	$l=2, g_3$	$l=2, g_4$	$l=2, g_5$	$l=2, g_6$
σ' (s^{-1})	4.194(−12)	−8.57 (−13)	−1.949 (−13)	4.019(−11)	−3.75 (−13)	9.56 (−10)	4.854(−13)	1.064(−11)	1.227(−11)
I_s	−8.136(−13)	−1.67 (−12)	−7.12 (−13)	−3.69 (−13)	−1.855(−12)	−8.47 (−13)	−9.48 (−13)	−4.09 (−13)	−6.47 (−13)
$I_{R,r}$	7.376(−12)	−9.22 (−13)	−2.665 (−12)	+1.397(−11)	2.377(−12)	1.044(− 9)	3.20 (−12)	9.653(−12)	9.646(−12)
$I_{C,r}$	6.106(−14)	+2.59 (−13)	−8.84 (−14)	−5.92 (−14)	−4.93 (−13)	−5.27 (−14)	−1.58 (−13)	−8.34 (−14)	−1.51 (−13)
$I_{R,nr}$	−2.107(−12)	−1.151(−11)	−7.078 (−12)	−4.616(−11)	−1.496(−12)	−7.98 (−11)	−1.411(−12)	−6.965(−12)	−7.669(−12)
$I_{C,nr}$	−9.891(−13)	−3.46 (−13)	−8.53 (−13)	−4.67 (−13)	−4.03 (−13)	−2.74 (−13)	−7.72 (−13)	−3.71 (−13)	−6.30 (−13)
I_F	1.864(−13)	1.236(−11)	1.0834(−11)	7.390(−11)	1.117(−12)	−1.626(−11)	2.629(−13)	8.700(−12)	1.153(−11)
I_L	5.024(−13)	9.76 (−13)	3.71 (−13)	2.20 (−13)	3.776(−13)	2.89 (−13)	3.09 (−13)	1.16 (−13)	1.80 (−13)
$I^{\mu}_{R,r}$	2.44 (−12)	−4.69 (−12)	−5.08 (−13)	−4.72 (−12)	1.113(−12)	6.01 (−12)	2.71 (−13)	2.63 (−12)	2.611(−12)
$I^{\mu}_{R,nr}$	−1.702(−14)	−1.46 (−13)	−3.34 (−13)	−1.43 (−13)	−1.83 (−13)	−2.62 (−13)	−3.81 (−13)	−3.50 (−14)	−8.65 (−14)

the integration range covering the region with $d\mu/dr \neq 0$. Table IV also shows that $I^{\mu}_{K,r}$ and $I^{\mu}_{K,nr}$ never dominate the other terms and if I_ε was set equal to zero all models would be stable. Therefore, the region with a superadiabatic temperature gradient leads in fact to an instability but only when the balance between all the I's is very critical because of the peculiar behaviour of the eigenfunction.

The magnitude of the destabilizing influence of the inhomogeneous zone seems nevertheless important for the occurence of an instability since in model 4, Δq_{st} is large enough to reduce significantly the destabilizing effect of the region of varying μ, leading to a stable $l=2$, g_4 mode. Moreover, the same analysis has been done for an 8 $M_\odot$ star and no instability was found.

5. Conclusion

Kato's mechanism can destabilize only models of low enough central hydrogen abundance. Therefore, if this mechanism were the only agent responsible for the formation of semi-convective zones, semi-convection could not exist during the early Main Sequence phases. Moreover, in more evolved models the chemical profile would only be very slightly altered since a small decrease of $\nabla_T - \nabla_{a,T}$ would be sufficient to restore stability.

This does not mean that we have to revise our views concerning the structure of semi-convective zones. In fact, the mechanism proposed by Gabriel (1970) is proving more efficient and since it leads to $\nabla_T = \nabla_{a,T}$, the instability found here will not be encountered and Kato's mechanism will not contribute to the formation of semi-convective zones.

References

Aure, J. L.: 1971, *Astron. Astrophys.* **11**, 345.
Boury, A., Gabriel, M., Ledoux, P., Noels, A., and Scuflaire, R.: 1975, *Astron. Astrophys.* **41**, 279.
Gabriel, M.: 1969, *Astron. Astrophys.* **1**, 321.
Gabriel, M.: 1970, *Astron. Astrophys.* **6**, 124.
Gabriel, M., Noels, A., Scuflaire, R., and Boury, A.: 1975a, *Mem. Soc. Roy. Sci. Liège*, 6 série, **8**, 273.
Gabriel, M., Scuflaire, R., Noels, A., and Boury, A.: 1975b, *Astron. Astrophys.* **40**, 33.
Ledoux, P. and Walraven, T.: 1958, *Hdb. Phys.* **LI**, 353.
Kato, S.: 1966, *Publ. Astr. Soc. Japan* **18**, 374.
Smeyers, P.: 1966, unpublished.
Scuflaire, R.: 1974, *Astron. Astrophys.* **37**, 449.
Tayler, R. J.: 1969, *Monthly Notices Roy. Astron. Soc.* **144**, 231.